



HAL
open science

Influence of thin-rimmed/-webbed gears on transmission dynamic behaviour-Approximate dynamic factor formula

Béregère Guilbert, Philippe Vexé

► To cite this version:

Béregère Guilbert, Philippe Vexé. Influence of thin-rimmed/-webbed gears on transmission dynamic behaviour-Approximate dynamic factor formula. *Forschung im Ingenieurwesen/Engineering Research*, 2021, 86 (3), pp.315-320. 10.1007/s10010-021-00543-1 . hal-03660204

HAL Id: hal-03660204

<https://hal.science/hal-03660204>

Submitted on 15 May 2023

HAL is a multi-disciplinary open access archive for the deposit and dissemination of scientific research documents, whether they are published or not. The documents may come from teaching and research institutions in France or abroad, or from public or private research centers.

L'archive ouverte pluridisciplinaire **HAL**, est destinée au dépôt et à la diffusion de documents scientifiques de niveau recherche, publiés ou non, émanant des établissements d'enseignement et de recherche français ou étrangers, des laboratoires publics ou privés.



Distributed under a Creative Commons Attribution - NonCommercial 4.0 International License

Influence of thin-rimmed/-webbed gears on transmission dynamic behaviour—Approximate dynamic factor formula

B. Guilbert¹  · P. Velex¹

Abstract

The objective of this paper is to analyse the effect of thin-webbed/-rimmed and consequently flexible gear bodies on dynamic tooth loads. To this end, an approximate dynamic factor formula is used, which makes it possible to estimate dynamic mesh force amplifications from Finite Element models, strain energies and quasi-static transmission errors. It is shown that, whenever solid gears are considered, the dynamic factor derived from the complete FE model results agrees well with those given by the analytical formula. When thin-rimmed/webbed gears are considered, the outcomes from the approximate dynamic factor formula are still in reasonable agreement with those of the complete FE model although the influence of rotating gear body cannot be accounted for. This good agreement also reveals that, for the tested geometries, dynamic couplings between dynamic mesh forces and gear body elasticity remain moderate.

Einfluss von dünnstegigen/-berandeten Zahnradern auf das dynamische Verhalten des Getriebes – Näherungsweise Formel für den Dynamikfaktor

Zusammenfassung

Ziel dieser Arbeit ist es, den Einfluss von dünnstegigen/-berandeten und damit flexiblen Zahnradkörpern auf dynamische Zahnbelastungen zu analysieren. Dazu wird eine näherungsweise dynamische Faktorformel verwendet, die es ermöglicht, dynamische Zahnkraftungen aus Finite-Elemente-Modellen, Dehnungsenergien und quasistatischen Übertragungsfehlern abzuschätzen. Es wird gezeigt, dass bei der Betrachtung von Vollzahnradern der aus den vollständigen FE-Modellergebnissen abgeleitete dynamische Faktor gut mit dem durch die analytische Formel angegebenen übereinstimmt. Bei der Betrachtung von dünnrandigen/stegigen Zahnradern stimmen die Ergebnisse der angenäherten dynamischen Faktorformel noch einigermaßen mit denen des vollständigen FE-Modells überein, obwohl der Einfluss des rotierenden Zahnradkörpers nicht berücksichtigt werden kann. Diese gute Übereinstimmung zeigt auch, dass für die getesteten Geometrien die dynamischen Kopplungen zwischen dynamischen Eingriffskräften und Radkörperelastizität moderat bleiben.

1 Introduction

The vast majority of the gear dynamics models are based on rigid discs connected by a time-varying elastic mesh interface [1–5]. Recently, however, efforts have been made to account for gear body flexibility. Li [6–8] built a full FE model of lightweight gears and studied the influence of the corresponding additional deflections on tooth contact con-

ditions. Parker et al. [9] used an elastic ring on constant stiffness foundation for flexible ring-gears and developed a 2D spur gear model combining finite element and analytical models [10]. Still in the context of planetary gears, Abousleiman et al. [11] inserted the results of condensed 3D finite element models of planet-carriers whereas Wu and Parker [12] used the thin ring theory to account for ring gear elasticity. Bettaieb et al. [13] and Liu et al. [14] included a condensed 3D finite element of gear body into spur and helical gear models. In this paper, the semi-analytical formulation of the dynamic factor for mesh forces proposed by Velex and Ajmi [15, 16] is revisited in the context of models integrating gear body flexibility. The formula was initially established for solid gears under the conditions of

✉ B. Guilbert
berengere.guilbert@insa-lyon.fr

¹ LaMCoS—INSA de Lyon, 27 bis Avenue Jean Capelle, 69621 Villeurbanne, France

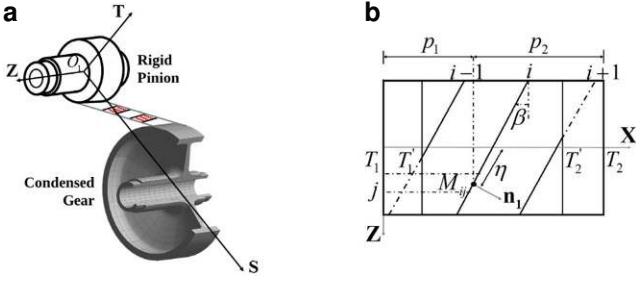


Fig. 1 a Hybrid gear model and b base plane [18]

small relative variations of mesh stiffness, hence mainly for helical gears, and linear behaviour (no contact losses). Within this domain of validity, the results from the dynamic factor formula are critically assessed and confronted with those delivered by the hybrid gear dynamic models proposed in [17, 18], which can capture the static and modal contributions of thin-rimmed/-webbed gears.

2 Model presentation—analytical dynamic ratio formula

2.1 Hybrid dynamic model

The modular hybrid gear dynamic model (Fig. 1a) includes lumped parameter and finite elements. It is assumed that all the contacts between the teeth occur on the theoretical line of actions in the base plane (Fig. 1b), which are discretised into small segments centred on the potential points of contact M_{ij} , where subscript i refers to the line of contact and j to the segment. A local stiffness k_{ij} [19] is attributed to every ij segment and distributed along the contact lines, making it possible to connect the pinion and gear degrees-of-freedom by a time-varying, possibly non-linear, Winkler foundation representative of the mesh interface elasticity [17]. The mechanical environment is simulated by combining lumped parameter and shaft elements along with substructures (super-elements), which account for gear body contributions [20] as illustrated in Fig. 1a in the particular case of a thin-rimmed gear. The corresponding state equations are solved by a time-step Newmark's integration scheme combined with a unilateral contact algorithm verifying that all contact forces on the mating teeth are compressive [3].

2.2 Dynamic ratio approximate formula

The gear dynamic factor formula in [16] is based on a classical 3D shaft finite element—lumped parameter dynamic model with rigid body gears [3]. Assuming that the relative mesh stiffness variation is small, a main order approxima-

tion of the instant dynamic factor is derived under the form [16]:

$$r \cong 1 + \sum_k \sqrt{\rho_k} \frac{k_{\phi k}}{k_m} Z(k) \quad (1)$$

with

Q_k and $k_{\phi k}$, the percentage of modal strain energy in the mesh interface and the modal stiffness respectively for Φ_k , k th mode shape obtained with a time-averaged stiffness matrix (over one mesh period in this paper),

k_m ,

the average (scalar) mesh stiffness

$Z(k)$,

the contribution of the k th mode shape to the dynamic response when considering transmission error-based excitations, i.e.,

$$Z(k) = \sum_{n \geq 1} \frac{\bar{A}_n^* \left[\left(\frac{\ddot{O}_k}{n} \right)^2 - 1 \right] + 2\bar{B}_n^* \xi_k \left(\frac{\ddot{O}_k}{n} \right)}{\left[\left(\frac{\ddot{O}_k}{n} \right)^2 - 1 \right]^2 + 4\xi_k^2 \left(\frac{\ddot{O}_k}{n} \right)^2} \sin n\vartheta + \frac{\bar{B}_n^* \left[\left(\frac{\ddot{O}_k}{n} \right)^2 - 1 \right] - 2\bar{A}_n^* \xi_k \left(\frac{\ddot{O}_k}{n} \right)}{\left[\left(\frac{\ddot{O}_k}{n} \right)^2 - 1 \right]^2 + 4\xi_k^2 \left(\frac{\ddot{O}_k}{n} \right)^2} \cos n\vartheta \quad (2)$$

where

- ξ_k is the damping factor of mode k
- $\vartheta = \Omega_1 t$, is an angular position (Ω_1 constant pinion rotation speed)
- $\ddot{O}_k = \frac{1}{\Omega_1} \sqrt{\frac{k_{\phi k}}{m_{\phi k}}}$, $k_{\phi k}$ and $m_{\phi k}$ modal stiffness and mass, is the k th natural frequency (with time-averaged mesh stiffness)
- $\bar{A}_n^* = \frac{A_n^*}{v_{x0}}$ and $\bar{B}_n^* = \frac{B_n^*}{v_{x0}}$, with v_{x0} the average static mesh deflection, are the dimensionless coefficients derived from transmission errors as:

$$\Gamma_k T E_S'' = - \sum_{n \geq 1} n^2 [A_n^* \sin n\vartheta + B_n^* \cos n\vartheta] \quad (3)$$

$\Gamma_k = \frac{\cos \beta_b}{v_{x0}} \frac{(\phi^T \mathbf{M} \widehat{\mathbf{X}}_0)_{/k}}{m_{\phi k}}$, $\widehat{\mathbf{X}}_0 = \bar{\mathbf{K}}^{-1} F_S \mathbf{V}$, $\bar{\mathbf{K}}$ averaged stiffness matrix, F_S static mesh force,

$T E_S''$ is the second order derivatives (with respect to ϑ) of the quasi-static transmission error under load. In contrast with [16], the no-load transmission error does not appear in the present study as it has been conducted without any errors or tooth modifications.

Fig. 2 Aeronautical transmission, **a** solid pinion and **b** lightweight gear

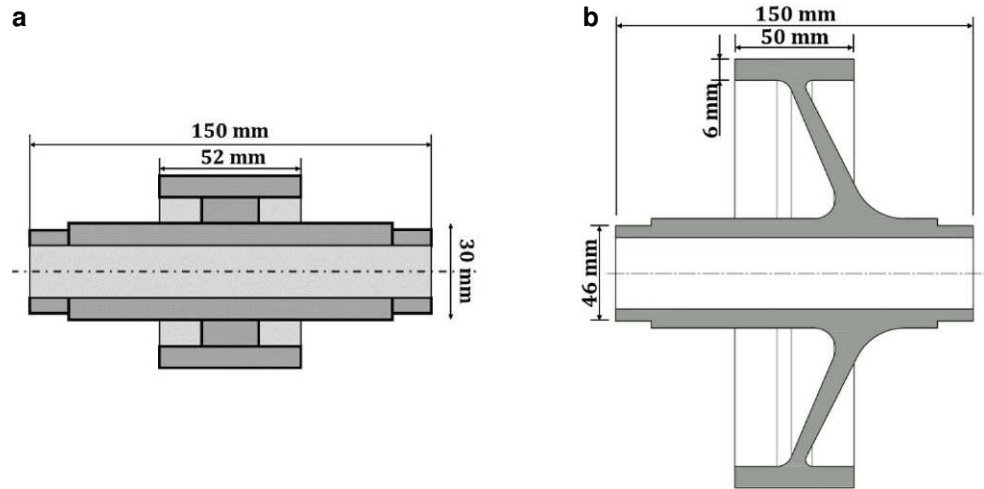
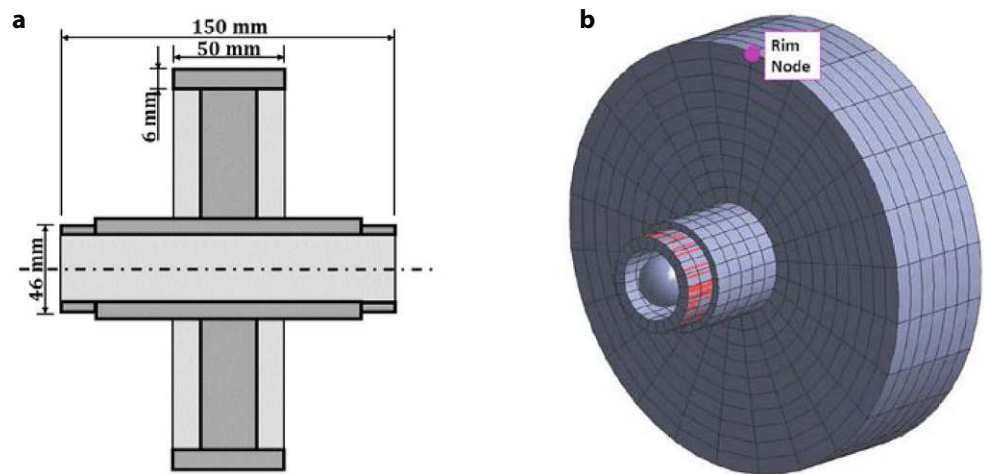


Fig. 3 Solid gear for validation purposes, **a** solid gear geometry and **b** 3D FEM model to be used in the hybrid dynamic model



3 Elements of validation

3.1 Test case definition

The test case defined in Fig. 2 is an aeronautical power transmission with a solid pinion and a lightweight gear. The pinion torque is 400 Nm and the gear data are in Table 1.

Table 1 Gear data

	Pinion	Gear
Module m (mm)	2.5	
Number of teeth	29	71
Pressure Angle ($^\circ$)	25	
Helix Angle ($^\circ$)	14	
Addendum coefficient	1	
Dedendum coefficient	1.25	
Profile shift coefficient	0.275	0.320
Fillet Radius/module	0.25	
Rim width b (mm)	52	50

3.2 Solid gear

For validation purposes, the original lightweight gear is replaced in the section by the solid gear shown in Fig. 3.

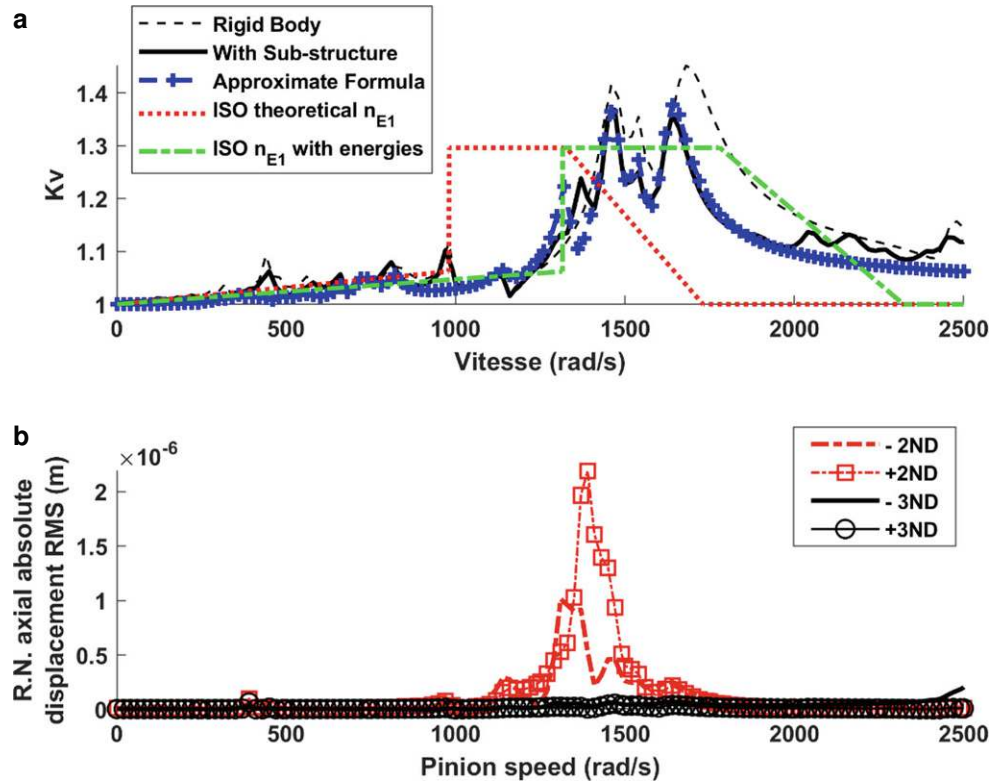
The modes with the highest percentages of strain energy stored in the mesh interface are listed in Table 2. These modes are those which contribute mostly to dynamic tooth forces hence to the dynamic factor. Most of them are bending modes for the pinion shaft, as their maximum energy is stored in the beam elements of the pinion. The 4th mode corresponds to a 2 Nodal Diameter (2N.D.) mode for the gear [22], showing that even solid gears can contribute to dynamic tooth loads via their deformable bodies. It can be noticed, however, that the dominant modes for mesh forces are mainly those which would be obtained by considering rigid discs, thus validating this modelling option for solid pinions and gears.

The dynamic responses in Fig. 4 have been calculated between 0 and 2500 rad/s on the pinion shaft. Two different parameters are represented versus speed, which are the

Table 2 Modal strain energy percentages (above 5% in the mesh interface), only the modes with more than 20% of the total strain energy in the mesh interface are kept for n_{E1} ISO 6336-1:2006 calculation [21]

Mode Number	Pinion Speed (rad/s)	Mode Frequency (Hz)	Strain Energy (%)				Mode Nature
			Mesh	Bearings	Shaft 1	Shaft (+gear body) 2	
1	1633	7536	26	19	54	10	Bending
2	1463	6754	23	16.6	40	20	Bending
3	1147	5295	18	33	40.5	8.7	Bending
4	1327	6129	7	2.7	4	86	2 <i>N.D.</i>
5	1534	7082	6.8	32	57	3.7	Bending

Fig. 4 Approximate formula with 5 harmonics and 5% and more of energy



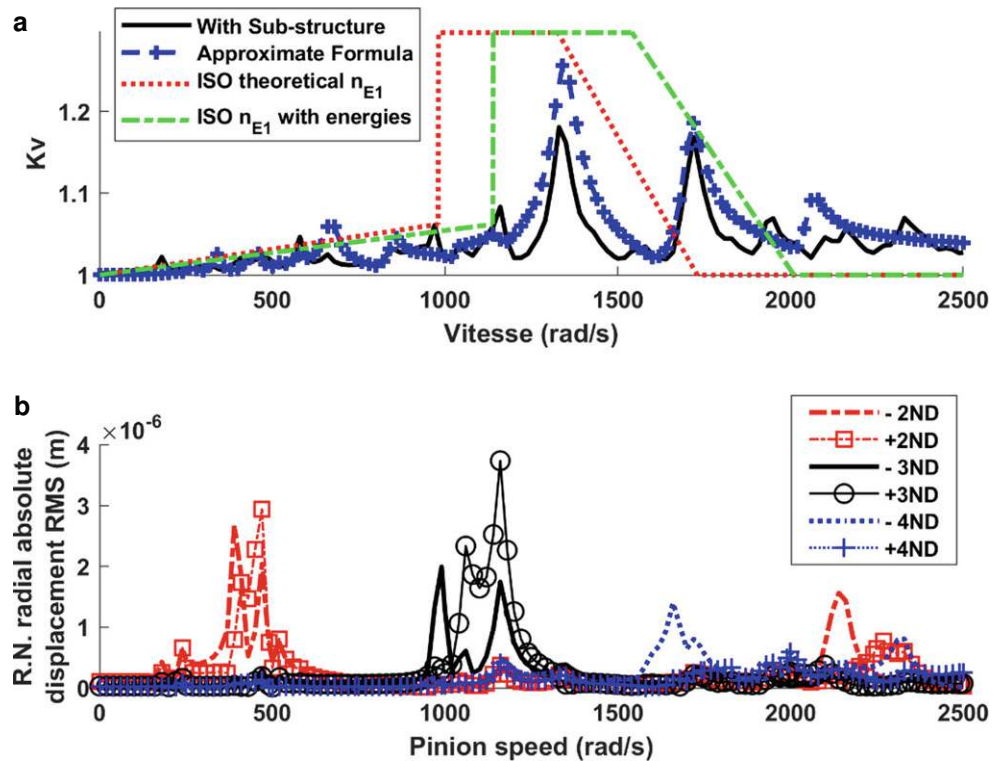
maximum dynamic factor R (maximum dynamic-to-static mesh force ratio at a given speed or the maximum of r defined in (2)) and the RMS of the axial displacement at the node on the gear rim shown in Fig. 3b. The dynamic factor has been calculated by numerical time integration of the hybrid model equations of motion (solid line) and by using the maximum of r derived from the approximate formula (2) (dotted line with cross marks) using the hybrid model modes (hence a deformable solid gear). A third curve has been superimposed (dotted line), which corresponds to the results obtained by assimilating the gear to a rigid disc. The dynamic factor using the ISO standard [21] with the theoretical critical speed n_{E1} given in [21] (red dotted curve in Fig. 4) and that obtained based on the modes with more than 20% of strain energy in the mesh interface (green dotted curve) have been added.

It can be noticed that the three first sets of results are very close. In this example of solid gear, the rigid disc or deformable gear body models give similar results but, as expected, the major critical speeds for tooth loading are slightly lower when gear flexibility is simulated. Interestingly, the approximate analytical dynamic factor calculated by keeping the few modes with more than 5% of strain energy in the mesh interface only (Table 2), agrees very well with the hybrid model results. Slight deviations can be observed with a peak around 1300–1400 rad/s, not reproduced by the analytical formula (2), which corresponds to a critical speed associated with gear body displacements as illustrated in Fig. 4b and the 2 ND mode in Table 2. The very limited couplings between mesh force and gear body modes probably explains the very good agreement between the analytical and numerical results in this example with a solid gear. The critical speed derived from the theoretical

Table 3 Strain energy distribution for modes with energy greater or equal to 5% in the meshing for the transmission with the thin-rimmed/webbed gear, only the modes with more than 20% of the total strain energy in the mesh interface are kept for n_{E1} ISO 6336-1:2006 calculation [21]

Mode Number	Pinion Speed (rad/s)	Mode Frequency (Hz)	Strain Energy (%)				Mode Nature
			Mesh	Bearings	Shaft 1	Shaft (+gear body) 2	
1	1340	6223	28	11	14	47	Coupled
2	1160	5363	14	20	23	43	Coupled +3N.D.
3	1730	7949	12	7	4	77	Coupled
4	480	2134	9	5	16	70	2N.D.
5	2180	9560	5	1	1	93	Degenerated 3N.D.

Fig. 5 Comparison between Dynamic Ratio (R) and R.N. radial displacement RMS over a speed range



ISO curve is not correctly positioned but the ISO dynamic factor formulae using the modes with maximum energy in the tooth mesh are better. For both curves, the amplitudes comparable reasonably well with those obtained by numerical simulations.

4 Analysis of the thin-rimmed/-webbed gear

Similar comparisons have been extended to the thin-rimmed/-webbed gear shown in Fig. 2. The corresponding percentages of modal strain energy in the mesh interfaces are given in Table 3. Because of the web flexibility, the 2N.D. gear body mode (number 4 in both Tables 2 and 3) has dramatically moved from 6129 to 2134Hz. The previous bending modes for the pinion shaft with the highest percentages of strain energy in the mesh obtained for a solid

gear are replaced by coupled modes affecting more components in the transmission, thus showing that highly flexible thin-rimmed/-webbed gears can influence dynamic tooth loads. These coupled modes still are the most energetic re the mesh interface, whereas gear body mode contributions remain limited.

The response curves in Fig. 5 show results of the same nature as those in Fig. 4 but for the thin-rimmed gear arrangement. In spite of the more complex interactions between the gear body and the mesh interface, the approximate formula (2) can still capture most of the dynamic tooth loads and particularly the two major response peaks. Some secondary peaks are not predicted by (2), which correspond to amplifications of gear body vibrations (see the second graph in Fig. 5) and are dynamically coupled to the mesh. Their amplitudes, however, remain limited. The displacement curve shows far more dynamic activity than in

the case of a solid gear, thus highlighting the role of coupled modes. The curves deduced from the ISO standard formulae [21] have been superimposed and it can be observed that they fail to correctly predict the dynamic mesh forces. The agreement is worse than compared with the solid gear example in Fig. 4, as expected based on the conditions of validity of the ISO formulae (for solid gears only).

5 Conclusions

A modular hybrid dynamic gear model which includes lumped parameters and 3D finite elements to account for the flexibility of thin-rimmed/-webbed gears has been used to assess the validity of the approximate formula of Velex and Ajmi [15, 16] to calculate mesh force dynamic factors. This formula is based on the hypotheses of the 3D rigid body gear model, and relies on the hypothesis of linear behaviour (no tooth contact losses) and small mesh stiffness time-variations (hence, more adapted to helical gears). The comparisons have been conducted on an aeronautical power transmission, by considering: a) a solid gear simulated as a rigid disc and by using 3D block finite elements and, b) the actual thin-rimmed, thin-webbed gear.

Overall, it seems that the analytical formula (2) can give a reasonable estimate of the dynamic mesh forces versus speed and can identify the major tooth critical speeds even for thin-rimmed applications. As expected, it fails to account for gear body mode contributions as it was developed in the context of pinions and gears assimilated to rigid discs connected by a time-varying elastic Winkler foundation. One major advantage of (2) is clearly the computational time as it only takes a few minutes for a complete response curve as opposed to days for the more involved hybrid model. It is therefore believed that this analytical formula can be useful at the early design stage and could probably be combined with the analytical formulations for transmission errors such as those proposed by in [23] in order to account for more realistic excitations including tooth shape deviations and errors.

Conflict of interest B. Guilbert and P. Velex declare that they have no competing interests.

References

1. Özgüven HN, Houser DR (1988) Mathematical models used in gear dynamics—A review. *J Sound Vib* 121(3):383–411
2. Kahraman A, Singh R (1990) Non-linear dynamics of a spur gear pair. *J Sound Vib* 142(1):49–75
3. Velex P, Maatar M (1996) A mathematical model for analysing the influence of shape deviation and mounting errors on gear behaviour. *J Sound Vib* 191:629–660

4. Vedmar L, Andersson A (2003) A method to determine dynamic loads on spur gear teeth and on bearings. *J Sound Vib* 267:1065–1084
5. Kubur M, Kahraman A, Zini DM, Kienzle K (2004) Dynamic analysis of a multi-shaft helical gear transmission by finite elements: model and experiment. *ASME J Vib Acoust* 126:398–406
6. Li S (2002) Deformation and bending stress analysis of a three-dimensional, thin-rimmed gear. *J Mech Des* 124:129–135
7. Li S (2013) Effects of centrifugal load on tooth contact stresses and bending stresses of thin-rimmed spurs gears and with inclined webs. *Mech Mach Theory* 59:34–47
8. Li S (2015) Effects of misalignment error, tooth modifications and transmitted torque on tooth engagements of a pair of spur gears. *Mech Mach Theory* 83:25–136
9. Parker RG, Sathe PJ (1999) Free vibration and stability of a spinning disk-spindle system. *J Vib Acoust* 121:391–396
10. Parker RG, Vijayakar SM, Imajo T (2000) Non-linear dynamic response of a spur gear pair: modelling and experimental comparisons. *J Sound Vib* 237:435–455
11. Aboislemman V, Velex P, Becquerelle S (2007) Modelling of spur and helical gear planetary drives with flexible gears and planet carriers. *J Mech Des* 129(1):95–106. <https://doi.org/10.1115/1.2359468>
12. Wu X, Parker RG (2008) Modal properties of planetary gear with an elastic continuum ring gear. *ASME J Appl Mech* 75:031014-1-12.
13. Bettaieb M, Velex P, Ajmi M (2007) A static and dynamic model of geared transmission by combining substructures and elastic foundations—Application on thin-rimmed gears. *J Mech Des* 129:184–194. <https://doi.org/10.1115/1.2406088>
14. Liu C, Zhao Y, Wang Y, Zhang T, Jia H (2021) Hybrid dynamic modelling and analysis of high-speed thin-rimmed gears. *ASME J Mech Des* 143:123401-1-13
15. Velex P, Ajmi M (2006) On the modelling of excitations in geared systems by transmission errors. *J Sound Vib* 290:882–909
16. Velex P, Ajmi M (2007) Dynamic tooth loads and quasi-static transmission errors in helical gears—Approximate dynamic factor formulae. *Mech Mach Theory* 42:1512–1526
17. Guilbert B, Velex P, Dureisseix D, Cutuli P (2016) A mortar based mesh interface for hybrid finite element/lumped parameter gear dynamic models—Application to thin-rimmed geared systems. *J Mech Des* 138:1233301-1-11
18. Guilbert B, Velex P, Dureisseix D, Cutuli P (2019) Modular hybrid model to simulate the static and dynamic behaviour of high-speed thin-rimmed gears. *J Sound Vib* 438:353–380
19. Weber C, Banaschek K (1953) Formänderung und Profilrücknahme bei Gerad- und Schrägverzahnten Antriebstechnik [Change in shape and profile modifications in spur and helical gears]. Vieweg, Braunschweig, p 11
20. Herting DN (1985) A general purpose, multi-stage component modal synthesis method. *Finite Elem Anal Des* 1:153–164
21. NF ISO 6336-1 (2006) Calculation of load capacity of spur and helical gears—Part 1: Basic principles, introduction and general influence factors
22. Guilbert B, Cutuli P, Velex P (2019) Hybrid models for the study of gear body dynamic deflections—Modes of the gear body. In: VDI International Conference on Gears, Garching, Germany, Sept. 18–20th, 2019
23. Velex P, Bruyère J, Houser DR (2011) Some analytical results on transmission errors in narrow-faced spur and helical gears – influence of profile modifications. *J Mech Des* 133:031010-1-11